CRYSTAL GROWTH & DESIGN
2007
VOL. 7, NO. 12
2517–2521

New Organic Nonlinear Optical Verbenone-Based Triene Crystal for Terahertz Applications

O-Pil Kwon,*,†,§ Seong-Ji Kwon,† Marcel Stillhart,† Mojca Jazbinsek,† Arno Schneider,† Volker Gramlich,‡ and Peter Günter†

Nonlinear Optics Laboratory, and Laboratory of Crystallography, ETH Zurich, CH-8093 Zurich, Switzerland

Received March 29, 2007

ABSTRACT: New organic nonlinear optical verbenone-based triene crystals have been developed, investigated and compared to analogous isophorone-based triene crystals studied previously. The verbenone-based crystals show molecular conformation and crystal structure similar to the analogous isophorone-based crystals and therefore retain large macroscopic nonlinearity and high thermal stability. However, other physical properties are improved; for example, the solubility in acetonitrile is about 2.5 times higher, and the melting temperature is about 13 °C lower, which are an advantage for solution and melt crystal growth, respectively. The verbenone-based crystals of sufficient size for bulk nonlinear optical applications, that is, $5 \times 4 \times 1.5$ mm^3, were successfully grown from acetonitrile solution by a slow evaporation method. Finally, terahertz (THz) absorption was measured in these crystals, and generation of THz waves was demonstrated.

Introduction

Organic nonlinear optical crystals are very promising for active integrated photonic devices[1,2] and terahertz (THz) applications.[3–7] Ultrashort electromagnetic pulses in the range of 0.1 to 10 THz have attracted numerous applications in spectroscopy and imaging due to their unique interactions with matter: harmlessness to biological cellular structures, high transmission in dielectrics (e.g., paper and plastics), and high absorbance in conducting materials (e.g., metals and semiconductors).[3] An attractive way to generate and detect THz waves is by using optical rectification and electro-optic sampling, respectively, which are limited most significantly by the nonlinear optical material used. The material requirements for such THz applications are sufficient macroscopic second-order nonlinearities and the possibility for velocity matching between the optical and the THz pulses. The latter is characterized by the coherence length l_c, which is intrinsically much longer in organic crystals compared to inorganic crystals.[7c] For 4′-dimethylamino-*N*-methyl-4-stilbazolium tosylate (DAST), which was shown to be a very efficient material for THz generation and detection[6,7] due to large nonlinear optical susceptibility and electro-optic coefficient,[8,9] the velocity-matching condition requires bulk crystals with an optimal thickness in the range of 0.1–1 mm.[7] On the other hand, single crystalline thin films with a thickness in the range of 0.2–10 μm are required for integrated photonic devices.[10] Therefore, the major challenge of organic nonlinear optical crystals for THz applications is to simultaneously achieve acentric packing of chromophores for large macroscopic nonlinearity and easy and practically reliable crystal growth yielding crystals of preferred orientation and morphology.

Organic configurationally locked polyene (CLP) crystals are of special interest due to large macroscopic nonlinearity and high thermal stability.[11,12] The isophorone-based CLP crystal DAT2 (2-{3-[2-(4-dimethylaminophenyl)vinyl]-5,5-dimethylcyclohex-2-enylidene} malononitrile, see Figure 1) exhibits large macroscopic nonlinearities with about 2 orders of magnitude greater second harmonic generation (SHG) efficiency than that of urea at 1.9 μm.[11] Moreover, the growth of high-quality single crystalline thin films of DAT2 was demonstrated by melt-based techniques.[11a,c] These films are very suitable for integrated photonics; however, for THz applications thicker crystals are desired. Here we present analogous verbenone-based DAV1 (2-{3-[2-(4-dimethylaminophenyl)vinyl]-6,6-dimethylbicyclo[3.1.1]hex-2-enylidene}malononitrile, Figure 1) crystals obtained by a chemical modification of the isophorone-based DAT2 crystal. DAV1 has modified crystal morphology and physical properties but still keeps the acentric packing of chromophores in the crystalline state (i.e., the large macroscopic nonlinearity). The physical, chemical, and structural properties of DAV1 crystals were characterized by UV/vis/near-infrared absorption spectroscopy, differential scanning calorimetry (DSC), thermogravimetric analysis (TGA), and X-ray diffraction measurements. We successfully grew bulk DAV1 crystals from acetonitrile solution by a slow evaporation method with a sufficient size of $5 \times 4 \times 1.5$ mm^3 for THz absorption and generation measurements.

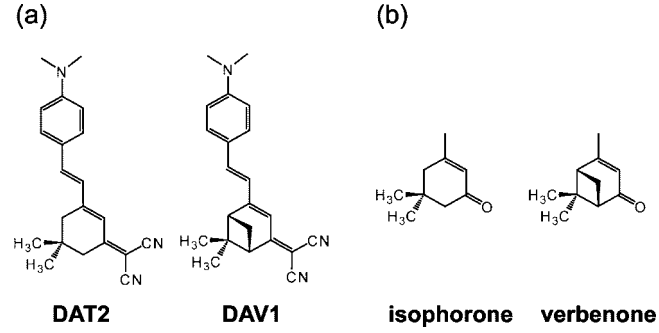

Figure 1. The chemical structures of the investigated isophorone-based DAT2 and verbenone-based DAV1 triene chromophores (a) and their starting materials for synthesis (b).

Experimental Section

Materials and Characterization. All chemicals were obtained from commercial suppliers (mainly from Aldrich). The DAV1 and DAT2

* Fax: +41 44 633 1056. Tel: +41 44 633 3295. E-mail: nlo@phys.ethz.ch, opilkwon@ajou.ac.kr.
† Nonlinear Optics Laboratory.
‡ Laboratory of Crystallography.
§ Present address: Department of Molecular Science and Technology, Ajou University, Suwon 443-749, Korea.

10.1021/cg070305q CCC: $37.00
Published on Web 11/09/2007

Table 1. Physical, Chemical, and Structural Properties of Verbenone-Based DAV1 and Isophorone-Based DAT2 Triene Chromophores

	λ_{max}[a] (nm)	T_m[b] (°C)	T_i[c] (°C)	powder SHG[d]	crystal system	point group	space group	ref
DAV1	505	220	278	1.1	monoclinic	2	$P2_1$	this work
DAT2	502	233	293	1.0	monoclinic	2	$P2_1$	ref

[a] λ_{max}: the wavelength of the maximum absorption in chloroform solution. [b] T_m: the melting temperature (peak position). [c] T_i: the thermal weight-loss temperature. [d] Powder SHG measured at a fundamental wavelength of 1.9 μm relative to that of DAT2 powder (about 2 orders of magnitude larger than that of urea).

Table 2. Summary of Crystallographic Data for the DAV1 and DAT2 Crystals

	DAV1	DAT2
formula	$C_{22}H_{23}N_3$	$C_{21}H_{23}N_3$
formula weight	329.43	317.42
crystal system	monoclinic	monoclinic
space group	$P2_1$	$P2_1$
a (Å)	6.5390(13)	6.1303(7)
b (Å)	7.4020(15)	7.4239(9)
c (Å)	19.450(4)	20.258(4)
α (deg)	90	90
β (deg)	98.82(3)	96.75(8)
γ (deg)	90	90
V (Å^3)	930.3(3)	915.6(2)
Z	2	2

chromophores and their intermediates were synthesized by Knoevenagel condensations according to the literature.[11,13] The intermediates were prepared by the condensation of isophorone or (1*S*)-(−)-verbenone with malononitrile using ammonium acetate and were then used for the second condensation with 4-dimethylaminobenzaldehyde. The materials were purified by recrystallization in a methylenechloride/methanol mixture solution. UV/vis/near-infrared absorption spectra were recorded by a Perkin-Elmer Lambda 9 spectrometer. Thermal measurements were carried out using a Perkin-Elmer TGA-7 and DSC-7 spectrometer (10 °C/min scan rate). The physical properties of the investigated chromophores are given in Table 1.

X-ray Crystal Structure Analysis. Single crystal X-ray diffraction experiments were carried out on a single crystal X-ray diffractometer equipped with a CCD detector (Xcalibur PX, Oxford Diffraction) with 65-mm sample–detector distance.[11] Data reduction and numerical absorption correction were performed using the software package CrysAlis.[14] The crystal structures were solved by direct methods, and the full data sets were refined on F^2, employing the programs SHELXS-97 and SHELXL-97.[15] Crystallographic data of acentric single crystal structures for DAV1 (CCDC 621008) and DAT2 (CCDC 278087) are given in Table 2.

Powder SHG Measurements. For the Kurtz and Perry powder test,[16] we used a tunable output of an optical parametric amplifier pumped by an amplified Ti:sapphire laser.[11] After the materials were ground, the crystalline powder was put into a 1.00 mm Hellma UV quartz cell to give a constant sample thickness. The backscattered light at the second-harmonic wavelength (953.5 nm) was measured with a silicon photodiode that is not sensitive to the fundamental wavelength of 1907 nm due to the absorption edge of Si near 1.1 μm, and the contribution of third-harmonic signal was eliminated by appropriate filters.

THz Absorption and Generation. THz time-domain spectroscopy (THz-TDS) was used to measure the THz absorption of a DAV1 crystal with a thickness of 1.53 mm along the crystallographic *c*-axis, which was grown from acetonitrile solution. The setup used was similar to that described in ref 3. The THz pulses were generated by optical rectification and detected by THz-induced lensing in organic ionic DAST crystals[7a,b] using 150 fs laser pulses at a wavelength of 1.3 μm.

We generated THz pulses by the same principle directly in a DAV1 crystal with a thickness of 1.53 mm, using a pump laser wavelength of 1.4 μm. The laser beam was polarized along the crystallographic polar *b*-axis of DAV1 crystal. The generated THz pulses polarized along the same axis were then detected by electro-optic sampling in a ZnTe crystal. To obtain the undistorted THz waveform, the probe laser pulses were frequency-doubled to 0.7 μm to ensure velocity-matching within the ZnTe crystal.[7c]

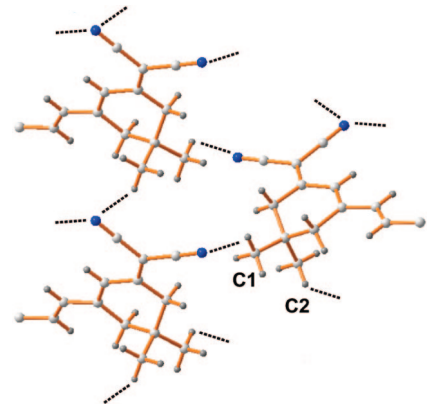

Figure 2. Schematic illustration of the supramolecular interactions of the ring part of isophorone-based triene DAT2 crystals. They form a three-dimensional network by weak hydrogen bonds C≡N···H−C, which are indicated by dotted lines.

The source of the laser pulses was an optical parametric generator/amplifier (Quantronix, TOPAS) which was pumped by a Ti:Sapphire laser with a repetition rate of 1 kHz and a central wavelength of 776 nm (Clark-MXR, CPA 2001). All experiments were carried out at room temperature, and the relative humidity of the surrounding air was kept below 5% to minimize the THz absorption of the ambient water vapor and hence to enhance the signal-to-noise ratio.

Results and Discussion

Design of Verbenone-Based Triene Crystal. The chemical structures of the isophorone-based DAT2 and the verbenone-based DAV1 triene chromophores investigated are shown in Figure 1 together with their abbreviations. Minor chemical modifications of the molecules often lead to large differences in the crystal structures: for example, CLP chromophores with the dimethylamino and the diethylamino groups exhibit noncentrosymmetric and centrosymmetric crystal structures, respectively.[11a,b] Therefore, careful modification of chemical structure is required for crystal engineering of CLP crystals.

Analogous unsaturated ring-typed isophorone (3,5,5-trimethyl-2-cyclohexen-1-on) and (1*S*)-(−)-verbenone (4,6,6-trimethylbicyclo[3.1.1]hept-3-en-2-one) are starting materials for synthesis of DAT2 and DAV1, respectively (see Figure 1b). As illustrated in Figure 2, the main supramolecular interactions of the isophorone-based DAT2 crystals are weak hydrogen bonds C≡N···H−C. The cyano (CN) groups act as hydrogen bond acceptor sites and H−C groups on the equatorial (labeled "C1") and axial (labeled "C2") methyl groups in the unsaturated ring part of the hexatriene bridge act as hydrogen bond donor sites.[11] Note that for DAT2 crystals the unsaturated ring-typed isophorone gives not only the configurationally locked polyene (CLP) but also the important hydrogen bond donor sites. Therefore, to retain the noncentrosymmetric molecular orientations in crystalline state, we want to keep the important hydrogen bond sites and their spatial positions when desining new CLP derivatives. In this work, we chose the introduction of (1*S*)-(−)-verbenone that has the same equatorial and axial methyl groups in the unsaturated ring part of isophorone but has an additional methyl bridge obtained by introducing a bicyclic system (see Figure 1).

Figure 3 shows the optimized conformations of the analogous isophorone and verbenone calculated through Molecular Mechanics with Cerius 2.[17] They were calculated by the DREIDING force field.[18] As shown in Figure 3c, the parts

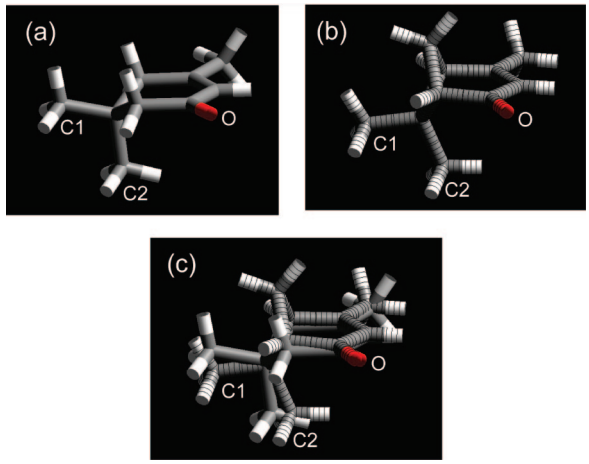

Figure 3. Optimized geometry of analogues calculated through Molecular Mechanics: isophorone (a), (1*S*)-(−)-verbenone (b), and their superimposition (c).

containing $CH_3-CH=CH-C=O$, which will form the π-conjugation part of DAT2 and DAV1 chromophores, show similar geometries. Therefore, we can expect that the chemical modification for obtaining the DAV1 chromophore will not affect considerably the microscopic molecular nonlinearity compared to the DAT2 chromophore. Moreover, the equatorial (C1) and axial (C2) methyl groups in the ring show similar positions. Therefore, we can also expect that the newly designed verbenone-based DAV1 crystals may show similar acentric crystal structure as the analogous isophorone-based DAT2 crystals. However, slightly different spatial positions of the equatorial (C1) and axial (C2) methyl groups may result in different physical properties.

Microscopic and Macroscopic Nonlinearity. Single crystal structure of DAV1 crystals grown from acetonitrile solution was determined by X-ray diffraction. The results of physical and structural measurements including melting temperature, thermal weight-loss temperature, the wavelength of maximum absorption, and crystallographic characteristics are given in Tables 1 and 2. Figure 4 shows the molecular structures of DAV1 and DAT2 molecules as determined by X-ray crystallography in the crystalline solid state. Both verbenone-based DAV1 and isophorone-based DAT2 molecules show very similar geometric conformations with a nearly planar π-conjugated bridge and similar positions of equatorial and axial methyl groups in the ring as expected from Molecular Mechanics calculations (Figure 3). Moreover, the wavelengths of maximum absorption λ_{max} in chloroform solution are also similar: 505 nm for DAV1 and 502 nm for DAT2 as listed in Table 1. Therefore, according to the similar molecular geometry and the so-called nonlinearity-transparency tradeoff,[1,2] the minor structural modification for obtaining the verbenone-based DAV1 crystals does not affect the large microscopic molecular nonlinearity of the isophorone-based DAT2 crystals.

DAV1 crystals grown from acetonitrile solution have a noncentrosymmetric crystal structure, monoclinic with space group symmetry $P2_1$ (point group 2). Compared to DAT2 crystals, DAV1 crystals show an analogous acentric crystal structure (i.e., the same space group symmetry, similar cell parameters, and crystallographic angles) with similar molecular orientations as shown in Figure 5. The cyano C≡N groups act as hydrogen bond acceptor sites and the CH groups on the equatorial and axial methyl groups in the ring part act as hydrogen bond donor sites. Resulting from the weak hydrogen

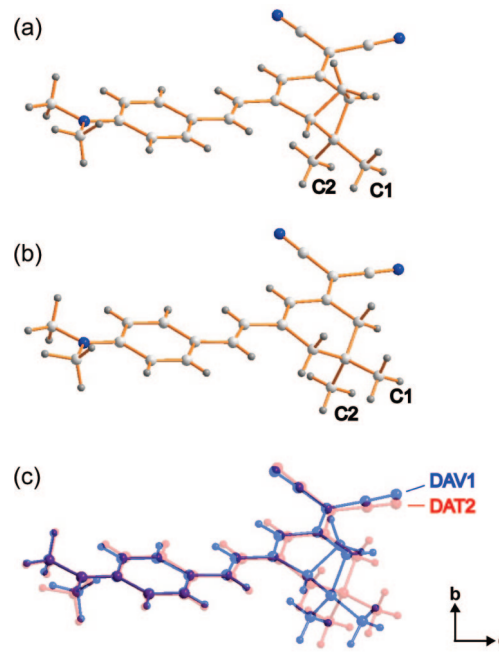

Figure 4. Molecular structures of the DAV1 (a) and DAT2 (b) as determined by X-ray crystallography in the crystalline state and their superimposition (c).

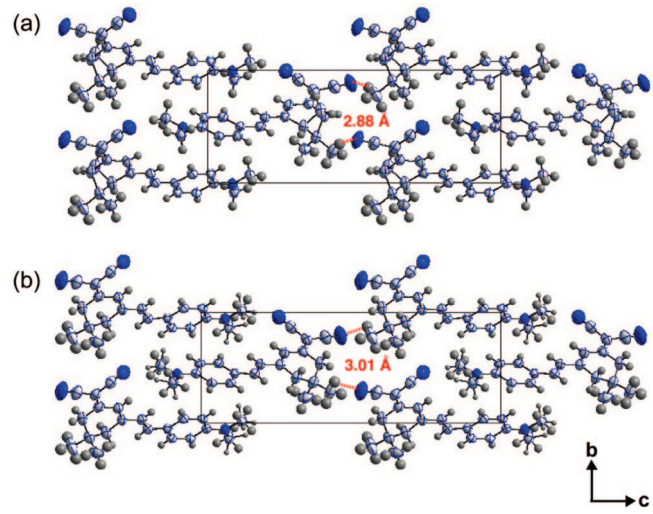

Figure 5. Crystal packing diagram projected along the *a*-axis for the monoclinic $P2_1$ phase of the DAV1 (a) and DAT2 (b) crystals. The dotted lines indicate hydrogen bonds formed by C≡N···H−C groups on equatorial methyl group (C1) in the unsaturated ring along the crystallographic *c*-axis: 2.88 Å for DAV1 (a) and 3.01 Å for DAT2 (b).

bonds of C≡N···H−C, the DAV1 molecules build a three-dimensional weak hydrogen-bonded network in the crystalline state like the DAT2 crystals (Figure 2).

In the Kurtz and Perry powder test[16] performed at a fundamental wavelength of 1.9 μm, DAV1 crystalline powder exhibits a slightly higher second harmonic generation (SHG) intensity than DAT2 powder, which is about 2 orders of magnitude larger than that of urea standard (see Table 1). The reason for the slightly higher macroscopic nonlinearity of DAV1 crystals may be related to the order parameter for chromophore orientation $\cos^3\theta_p$, where θ_p is the angle between the molecular charge transfer axis and the polar crystalline axis.[1] As shown in Figure 4c, the long axis of the DAV1 molecules, which is a

favorable direction of charge delocalization, is slightly more aligned along the crystallographic polar *b*-axis than for DAT2. Therefore, DAV1 crystals may exhibit a slightly higher macroscopic nonlinearity.

Variation of Physical Properties. Although similar crystal structures of DAV1 and DAT2 crystals lead to similar macroscopic nonlinearities, they possess different physical properties such as melting temperature and solubility. The thermal stabilities of chromophores were investigated using thermogravimetric analysis (TGA) and differential scanning calorimetry (DSC) under nitrogen atmosphere (scan rate: 10 °C/min). The thermal weight-loss temperature T_i, indicating either sublimation or decomposition of the chromophores is defined here at the intercept of the leading edge of the weight loss by the baseline of the TGA scans. The melting temperature T_m is defined here as the peak position in the DSC scan. The DAV1 chromophores exhibit a very high thermal stability with the thermal weight-loss temperature T_i of about 278 °C. They exhibit a large temperature difference of about 68 °C between the thermal weight-loss temperature T_i and the melting temperature T_m. By introducing the verbenone analogue, the melting temperature T_m of 220 °C for DAV1 decreases with respect to the isophorone-based DAT2 crystals (233 °C). The lower melting temperature, which is still high enough for good environmental stability, is an advantage for applying melt-based crystal growth techniques.

The CLP crystals are soluble in polar solvents such as acetone, acetonitrile and dimethylformamide, and a nonpolar solvent methylenechloride, while the solubility in methanol or ethanol is too low for growing bulk crystals. The solubility of DAV1 is about 0.5 g/100 g acetonitrile and the solubility of DAT2 is 0.2 g/100 g acetonitrile. Since these solubilities are still relatively low, the 2.5 times higher solubility of verbenone-based DAV1 crystals is an advantage for solution growth because of a better material transport leading to faster growth rate and/or larger crystal size.

Bulk Single Crystals. Bulk single crystals of DAV1 were obtained by the slow evaporation method in acetonitrile solution. Figure 6a shows as-grown crystals with sizes of about 5 × 4 × 1.5 mm^3. DAV1 crystals grow into two-dimensional platelike crystals with large surfaces along (001) crystallographic plane and edges along [010] and [100] crystallographic vectors as illustrated in Figure 6a. The grown DAV1 crystals are much thicker, with thicknesses of millimeter scale along the *c*-axis, compared to similarly grown DAT2 crystals with thicknesses of less than 50 μm.[11] The reason for thicker DAV1 crystals may be related to the shorter distances of hydrogen bonds formed by C≡N···H−C groups on the equatorial methyl group (C1) in the ring along the crystallographic *c*-axis: 2.88 Å for DAV1 and 3.01 Å for DAT2 (see Figure 5). The shorter distances of the hydrogen bonds result in a shorter length of the unit cell along the *c*-axis as in DAT2 crystals: 19.450(4) Å for DAV1 and 20.258(4) Å for DAT2 as listed in Table 2. Therefore, in DAV1 crystals the interaction between the molecules along the *c*-axis is stronger, and therefore the growth rate along the *c*-axis is faster than in DAT2 crystals.

We measured transmission of an as-grown unpolished DAV1 crystal (c-plate with a thickness of 1.53 mm) for the incident light polarized parallel to the crystallographic *a*- and *b*-axis in the visible and near-infrared regions as shown in Figure 6b. Measuring at different positions of the sample results in an identical transmittance curve. As-grown DAV1 crystals are therefore optically homogeneous. As shown in figure 6b, DAV1 crystals exhibit a strong anisotropy; the transmittance along the

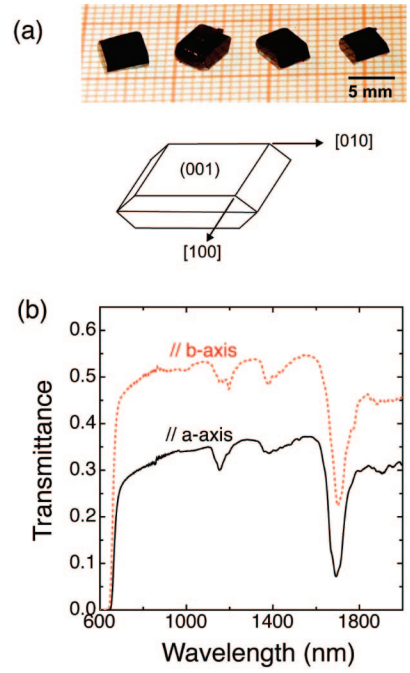

Figure 6. (a) Photograph of DAV1 crystals grown by the slow evaporation method in acetonitrile. (b) Transmission spectra of an as-grown unpolished DAV1 crystal (c-plate) with a thickness of 1.53 mm for the incident light polarized parallel to the crystallographic *a*- and *b*-axis.

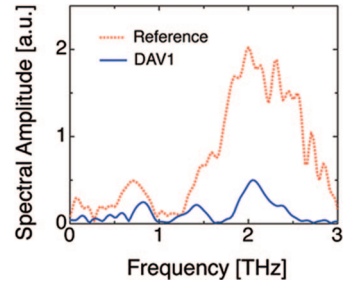

Figure 7. THz absorption spectra of the unpolished DAV1 crystal with thickness of 1.53 mm: the reference THz spectrum emitted from DAST without a sample in place (dotted line) and a measurement with the DAV1 crystal (solid line).

a-axis is significantly lower than along the *b*-axis. Therefore, the refractive index and the absorption constant along the *a*-axis are higher than along the *b*-axis, which is because the long axes of the DAV1 molecules are closer to the *a*-axis than to the *b*-axis.

THz Absorption and Generation. The reference THz spectrum that was used to characterize DAV1 crystals is shown by the dotted line in Figure 7 and was emitted from an organic ionic DAST crystal with a thickness of 0.4 mm by optical rectification, covering the spectral range between 0.5 and 3 THz. The THz pulses were detected by THz-induced lensing in DAST crystals.[7b] The strong absorption at 1.1 THz is due to a transverse optical phonon in DAST, while the smaller lines stem from remaining ambient water vapor absorption. The solid line represents a measurement with the unpolished as-grown DAV1 crystal with a thickness of 1.53 mm in the THz beam path. Both Fresnel losses at the crystal surfaces and THz absorption due to impurities reduce the measured THz amplitude, but since these effects are expected to be nearly frequency independent, one can clearly identify a strong absorption at 1.6 THz, which

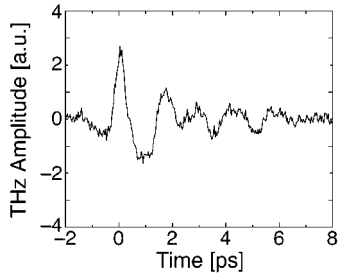

Figure 8. THz pulse generated through optical rectification in a 1.53-mm-thick unpolished DAV1 crystal using a pump laser wavelength of 1.4 μm and detected by electro-optic sampling in a ZnTe crystal.

is attributed to an optical phonon of DAV1. Furthermore, the result leads to the conclusion that DAV1 is not transparent between 2.5 and 3 THz, but this observation has to be verified in further experiments with a larger THz bandwidth.

Figure 8 shows that DAV1 may be used as a THz source. The as-grown unpolished DAV1 crystal with a thickness of 1.53 mm was used with a laser wavelength of 1.4 μm. The curve renders a few-cycle THz pulse as it is typical for optical rectification. The pulses were detected by electro-optic sampling in a ZnTe crystal. Note that the generation conditions are not optimized yet; the THz amplitude may be enhanced once the geometry and the velocity-matching conditions are optimized. On the basis of the results of the powder SHG efficiency of DAV1 crystals, we expect that these improved measurements will reveal DAV1 to be an efficient THz source.

Conclusions

We have reported on new organic nonlinear optical verbenone-based triene DAV1 crystal that was designed to improve physical properties compared to the analogous isophorone-based triene DAT2 crystal studied previously. The verbenone-based DAV1 crystals show molecular conformation and crystal structure similar to the isophorone-based DAT2 crystals and therefore retain large macroscopic nonlinearities and high thermal stability. However, some other physical properties are improved; for example, the solubility is higher and the melting temperature is lower, which are of advantage for solution and melt crystal growth, respectively. DAV1 crystals of $5 \times 4 \times 1.5$ mm^3 size were successfully grown in acetonitrile solution by the slow evaporation method, which is of sufficient size for bulk nonlinear optics including THz applications. In THz absorption measurements, we observed a strong absorption at 1.6 THz, which is attributed to a polar transverse optical phonon of DAV1. We also demonstrated THz generation using an as-grown and unpolished DAV1 crystal as a THz source. Further studies will focus on optimizing the geometry and velocity-matching condition for enhancing the efficiency for THz wave generation.

Acknowledgment. This work was supported by the Swiss National Science Foundation.

References

(1) (a) Jazbinsek, M.; Kwon, O. P.; Bosshard, Ch.; Günter, P. In *Handbook of Organic Electronics and Photonics*; Nalwa, S. H. Ed.; American Scientific Publishers: Los Angeles, 2007. (b) Bosshard, Ch.; Bösch, M.; Liakatas, I.; Jäger, M.; Günter, P. In *Nonlinear Optical Effects and Materials*; Günter, P. Ed.; Springer-Verlag: Berlin, 2000. (c) Bosshard, Ch.; Sutter, K.; Prêtre, Ph.; Hulliger, J.; Flörsheimer, M.; Kaatz, P.; Günter, P. In *Organic Nonlinear Optical Materials, Volume 1 of Advances in Nonlinear Optics*; Gordon and Breach Science Publishers: New York, 1995.

(2) (a) Nalwa, H. S.; Miyata, S. In *Nonlinear Optics of Organic Molecules and Polymers*; CRC Press: Boca Raton, FL, 1997. (b) Marder, S. R. In *Materials for Nonlinear Optics: Chemical Perspectives, ACS Symposium Series*; American Chemical Society: Washington, DC, 1991. (c) Ma, H.; Jen, A. K. Y.; Dalton, L. R. *Adv. Mater.* **2002**, *14*, 1339.

(3) Ferguson, B.; Zhang, X. C. *Nat. Mater.* **2002**, *1*, 26.

(4) (a) Hashimoto, H.; Takahashi, H.; Yamada, T.; Kuroyanagi, K.; Kobayashi, T. *J. Phys.: Condens. Matter.* **2001**, *13*, L529. (b) Kuroyanagi, K.; Fujiwara, M.; Hashimito, H.; Takahashi, H.; Aoshima, S.; Tsuchiya, Y. *Jpn. J. Appl. Phys.* **2006**, *45*, 4068. (c) Carey, J. J.; Bailey, R. T.; Pugh, D.; Sherwood, J. N.; Cruickshank, F. R.; Wynne, K. *Appl. Phys. Lett.* **2002**, *81*, 4335.

(5) (a) Sinyukov, A. M.; Leahy, M. R.; Hayden, L. M.; Haller, M.; Luo, J.; Jen, A. K. Y.; Dalton, L. R. *Appl. Phys. Lett.* **2004**, *85*, 5827. (b) Zheng, X.; Sinyukov, A. M.; Hayden, L. M. *Appl. Phys. Lett.* **2005**, *87*, 081115. (c) Sinyukov, A. M.; Hayden, L. M. *J. Phys. Chem. B* **2004**, *108*, 8515. (d) Nahata, A.; Auston, D. H.; Wu, C.; Yardley, J. T. *Appl. Phys. Lett.* **1995**, *67*, 1358.

(6) (a) Zhang, X. C.; Ma, X. F.; Jin, Y.; Lu, T. M.; Boden, E. P.; Phelps, P. D.; Stewart, K. R.; Yakymyshyn, C. P. *Appl. Phys. Lett.* **1992**, *61*, 3080. (b) Kuroyanagi, K.; Yanagi, K.; Sugita, A.; Hashimoto, H.; Takahashi, H.; Aoshima, S.; Tsuchiya, Y. *J. Appl. Phys.* **2006**, *100*, 043117. (c) Taniuchi, T.; Okada, S.; Nakanishi, H. *J. Appl. Phys.* **2004**, *95*, 5984.

(7) (a) Schneider, A.; Neis, M.; Stillhart, M.; Ruiz, B.; Khan, R. U. A.; Günter, P. *J. Opt. Soc. Am. B* **2006**, *23*, 1822. (b) Schneider, A.; Biaggio, I.; Günter, P. *Appl. Phys. Lett.* **2004**, *84*, 2229. (c) Schneider, A.; Stillhart, M.; Günter, P. *Opt. Express.* **2006**, *14*, 5376.

(8) (a) Marder, S. R.; Perry, J. W.; Yakymyshyn, C. P. *Chem. Mater.* **1994**, *6*, 1137. (b) Pan, F.; Wong, M. S.; Bosshard, Ch.; Günter, P. *Adv. Mater.* **1996**, *8*, 592.

(9) Pan, F.; Knöpfle, G.; Bosshard, Ch.; Follonier, S.; Spreiter, R.; Wong, M. S.; Günter, P. *Appl. Phys. Lett.* **1996**, *69*, 13.

(10) (a) Jazbinsek, M.; Rabiei, P.; Bosshard, Ch.; Günter, P. *AIP Conf. Proc.* **2004**, *709*, 187. (b) Manetta, S.; Ehrensperger, M.; Bosshard, Ch.; Günter, P. *C. R. Phys.* **2002**, *3*, 449. (c) Swamy, R. K.; Kutty, S. P.; Titus, J.; Khatavkar, S.; Thakur, M. *Appl. Phys. Lett.* **2004**, *85*, 4025. (d) Leyderman, A.; Cui, Y. L. *Opt. Lett.* **1998**, *23*, 909. (e) Kaino, T.; Cai, B.; Takayama, K. *Adv. Funct. Mater.* **2002**, *12*, 599. (f) Geis, W.; Sinta, R.; Mowers, W.; Deneault, S. J.; Marchant, M. F.; Krohn, K. E.; Spector, S. J.; Calawa, D. R.; Lyszczarz, T. M. *Appl. Phys. Lett.* **2004**, *84*, 3729.

(11) (a) Kwon, O. P.; Ruiz, B.; Choubey, A.; Mutter, L.; Schneider, A.; Jazbinsek, M.; Gramlich, V.; Günter, P. *Chem. Mater.* **2006**, *18*, 4049. (b) Kwon, O. P.; Kwon, S. J.; Jazbinsek, M.; Choubey, A.; Losio, P.; Gramlich, V.; Günter, P. *Cryst. Growth Des.* **2006**, *6*, 2327. (c) Choubey, A.; Kwon, O. P.; Jazbinsek, M.; Günter, P. *Cryst. Growth Des.* **2007**, *7*, 402.

(12) (a) Kwon, S. J.; Kwon, O. P.; Jazbinsek, M.; Gramlich, V.; Günter, P. *Chem. Commun.* **2006**, 3729. (b) Kwon, O. P.; Kwon, S. J.; Jazbinsek, M.; Choubey, A.; Gramlich, V.; Günter, P. *Adv. Funct. Mater.* **2007**, *17*, 1750.

(13) (a) Shu, C. F.; Tsai, W. J.; Jen, A. K.-Y. *Tetrahedron Lett.* **1996**, *37*, 7055. (b) Ermer, S.; Lovejoy, S. M.; Leung, D. S.; Warren, H.; Moylan, C. R.; Twieg, R. J. *Chem. Mater.* **1997**, *9*, 1437.

(14) http://www.oxford-diffraction.com.

(15) (a) Sheldrick, G. *SHELXS-97. Program for the Solution of Crystal Structures*;University of Göttingen, Germany, 1997. (b) Sheldrick, G. *SHELXL-97. Program for the Refinement of Crystal Structures*; University of Göttingen, Germany 1997.

(16) Kurtz, S. K.; Perry, T. T. *J. Appl. Phys.* **1968**, *39*, 3798.

(17) Molecular Simulations Inc., 9685 Scranton Road, San Diego, CA.

(18) Mayo, S. L.; Olafson, B. D.; Goddard III, W. A. *J. Phys. Chem.* **1990**, *94*, 8897.

CG070305Q